Fabrication and Characterization of Pure and Well-Aligned Carbon Nanotubes Using Methane/Nitrogen−Ammonia Plasma

W. K. Wong, C. P. Li, F. C. K. Au, M. K. Fung, X. H. Sun, C. S. Lee, and S. T. Lee*

Center of Super-Diamond and Advanced Films (COSDAF) and Department of Physics and Materials Science, City University of Hong Kong, Hong Kong SAR, China

W. Zhu

Agere Systems, Inc. 600 Mountain Avenue, Murray Hill, New Jersey 07974

Received: July 11, 2002; In Final Form: November 11, 2002

Well-aligned multiwalled carbon nanotubes (CNTs) were grown by microwave plasma-enhanced chemical vapor deposition using N_2 and NH_3 as the carrier gases and CH_4 as the carbon source. Iron films with 1−5 nm thickness on silicon substrates acted as catalysts. Scanning electron microscopy revealed that the CNTs grew via the base growth mechanism at a rate ∼100 nm/s. Transmission electron microscopy showed that multiwalled CNTs had a "bamboo" structure, and the smallest CNTs of ∼6 nm in diameter were acquired on 1 nm Fe film. These "smallest" CNTs were comprised of amorphous structure, due to the formation of sp^3 C−H bonds as proven by Fourier transform infrared spectroscopy and electron energy loss spectroscopy, suggesting hydrogen incorporation during growth of CNTs. Without N_2 gas, no CNTs could be grown, while curly CNTs with poor alignment were grown with no NH_3. In both cases, high-purity CNTs with no CN_x impurities were obtained. Field electron emission revealed that the lowest turn-on and threshold fields were obtained from the CNTs grown on the 1 nm thick iron films on silicon substrate, i.e., 3.5 V/μm and 4.5 V/μm, respectively. Under an applied field of 7.5 V/μm, emission current density of 0.63 A/cm^2 can be obtained.

Introduction

Carbon nanotubes (CNTs) are potentially useful for a wide range of potential applications, including local probes for microscopy, nanoscale fillers, templates for growing 1D nanomaterials, hosts for energy storage, sensors, components in novel electronic devices, electron field emitters, etc.[1−6] To date, various methods have been used to fabricate single-walled or multiwalled CNTs. They include arc-discharge,[7−9] laser ablation,[10] and chemical vapor deposition (CVD).[11−15] The CVD method (thermal and microwave plasma-enhanced CVD) is capable of producing aligned CNTs via self-biasing (i.e., plasma induced)[14−16] or external biasing (i.e., dc biasing) of the substrate.[17−19] It is generally accepted that CNTs are produced via carbon precipitation in the supersaturated metal catalysts of iron, cobalt, nickel, etc., which reside either at the base (base growth mechanism) or tip (tip growth mechanism) of the CNTs.[20] The common carrier gases used in CVD for growing CNTs include hydrogen (H_2) and ammonia (NH_3) while the reactant gases are methane (CH_4) or acetylene (C_2H_2). Instead of H_2 and NH_3, N_2 is another carrier gas for growing CN_x nanomaterials. For example, Ma et al. synthesized CN_x/CNTs junctions by using a gas mixture of N_2/CH_4 and H_2/CH_4 in a continuous growth process.[21] Zhang et al. fabricated films of well-aligned carbon nitride nanotubes using N_2/CH_4 plasma.[18] Compared with the other two carrier gases, N_2 has the advantages of being nonpoisonous and economical.

Here we report well-aligned carbon nanotubes grown by using a microwave plasma-enhanced CVD method. Under the investigation of electron energy loss spectroscopy (EELS) and X-ray photoemission spectroscopy (XPS), we found that pure and well-aligned multiwalled carbon nanotubes free of CN_x compounds can be fabricated in a N_2-NH_3/CH_4 plasma. Moreover, the FEE properties were also studied; we found that these pure and well-aligned carbon nanotubes exhibited excellent FEE performance.

* Author to whom all correspondence should be addressed. E-mail: apannale@cityu.edu.hk.

Experimental Method

Carbon nanotubes were synthesized in a microwave plasma-enhanced CVD system (ULVAC: CN-CVD-100), where a 2.45 GHz microwave generator with 500 W power is used to create plasma and provide part of the substrate heating. The heating of the substrate for the pretreatment is supplied by a halogen photo optic lamp housed inside a graphite cage, which serves as the substrate holder, providing a uniform temperature distribution. The substrate temperature is measured by a pin-like thermocouples (Omega: K-type) introduced inside the graphite cage. The growing process is carried out inside a circular quartz tube chamber. The base pressure of the system is below 10 mTorr, which is maintained by a rotary pump. Prior to the growing process, a thin film of iron metal catalyst with a thickness of 1, 2, and 5 nm was deposited onto a silicon(111) substrate by electron beam deposition. The thickness of the film was monitored by a quartz microbalance associated with a thickness and rate controller. The Fe-coated samples were simultaneously transferred to the microwave CVD system in air such that all CNTs were deposited under the same experimental conditions. The samples were then heated to 500 °C by the halogen lamp in a hydrogen atmosphere with a gas flow rate and pressure of ∼80 sccm and ∼30 Torr, respectively. At

10.1021/jp026502b CCC: $25.00
Published on Web 01/24/2003

this time, the mixture of nitrogen and ammonia was introduced through the same mass flow controller into the chamber to completely replace the hydrogen gas. The plasma was started after adding methane. The total growth pressure was ~30 Torr with a gas ratio of $N_2/NH_3/CH_4$ =50:2:1. The growth of CNTs (black color) could be observed after the substrate temperature had reached ~850 °C. After growing for 2 min, the plasma was turned off and the samples were allowed to cool to room temperature in a hydrogen atmosphere.

The morphology of each sample was analyzed by utilizing SEM (Philips 30XL). The structure of CNTs was studied by high-resolution transmission electron microscopy (HRTEM) (Philip CM200FEG at 200 kV), while the structural and compositional analysis were done by electron energy loss spectroscopy (EELS) (Gatan GIF 200) in the HRTEM, Fourier transform infrared spectroscopy (FTIR), and X-ray photoemission spectroscopy (XPS) (VG ESCALAB 220i-XL with a monochromatic aluminum Kα source of 1486.6 eV). The TEM and EELS specimens were prepared by dispersing the CNTs in methanol and dropping the mixture onto copper microgrids.

The field emission characteristics were measured under a pressure of 2×10^{-8} Torr in a scanning-probe field emission system. A detailed description of this system can be found elsewhere.[22] The field emission I−V characteristics were measured at four different tip-to-sample distances (d), i.e., 100, 150, 200, and 250 μm. Five I−V measurements were taken for each distance d to ensure reproducibility. The effective emission area (A) used to calculate the current density is defined as $A = 2\pi Rd(2^{1/n} - 1)$,[23] where $n = (V/I)(\mathrm{d}I/\mathrm{d}V)$, where R is the radius of the anode probe.

Results and Discussion

Figure 1, parts a, b, and c, shows the SEM images of CNTs that were deposited on iron-coated silicon substrates with a film thickness of 5, 2, and 1 nm, respectively. The estimated density of the CNTs was ~10^9 cm^2. The lengths of CNTs were in the range of 6−12 μm. CNTs of 12 μm length were grown when the iron film thickness was 1 nm (Figure 1c), which corresponded to a growth rate of ~100 nm/s. In contrast, CNTs of only ~6 μm length could be grown when the iron film thickness was 5 nm with the same growth time (Figure 1a). The magnified SEM image of CNTs deposited on the 1 nm Fe film (Figure 1d) shows that CNTs with a smaller diameter are longer (shown in the rectangle) than those with a larger diameter (below the rectangle). This suggests that CNTs of smaller diameter could grow at a higher rate, and the growth of CNTs followed the constant mass deposition rate of carbon.[15] In our case, the difference in the diameter of CNTs arose from the nonuniformity of iron films deposited on the silicon substrate. A thinner region gave rise to Fe clusters of smaller size during pretreatment, which in turn led to the growth of CNTs with a smaller diameter. On the other hand, the alignment and the uniformity of the orientation to some extent could also be affected by the diameter of CNTs. From Figure 1a−d, except for the misalignment caused by scratches of tweezers, it is clear that the degree of CNTs alignment and the uniformity of their orientation become degraded with increasing Fe film thickness.[24] As the film thickness increases, the diameter of the grown CNTs also increases. CNTs with a smaller diameter may exhibit a higher sensitivity to the electric self-bias and consequently show better alignment, as the alignment of the present CNTs was apparently induced by the electric self-bias imposed on the substrate from the microwave plasma.[14]

TEM images in Figure 2 show that almost all the CNTs were multiwalled and had "bamboo"-type or polymerized nanobell

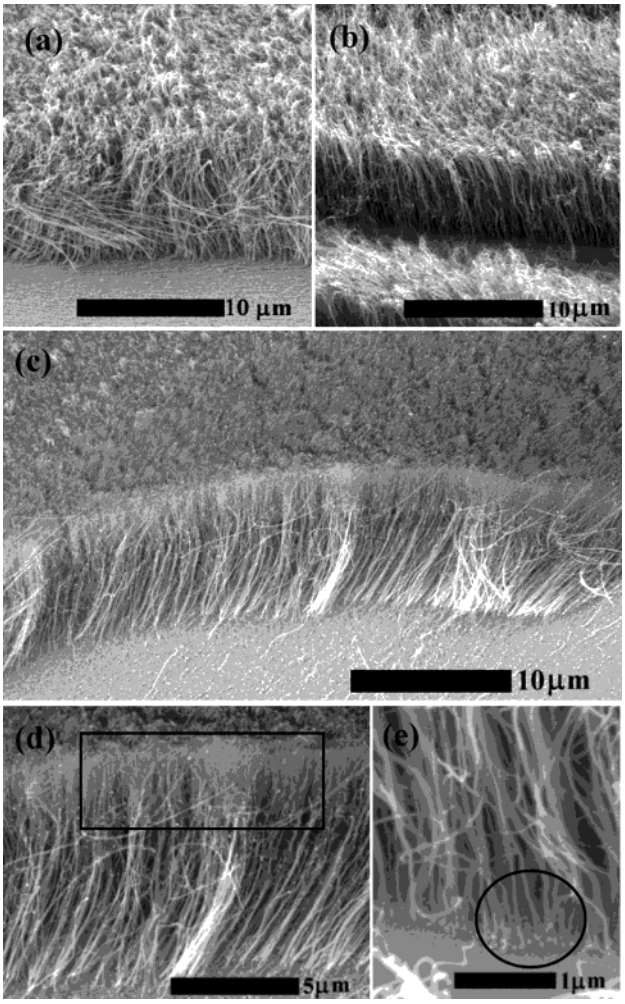

Figure 1. SEM of CNTs deposited on an Fe film of thickness (a) 5 nm, (b) 2 nm, and (c, d) 1 nm. (d) The magnified image shows that CNTs with a smaller diameter (in the rectangle) have a longer length than CNTs with a larger diameter (below the rectangle). (e) The Fe particles residing at the bottom suggested that CNTs were grown via the base growth mechanism.

structures [16,21,25] (Figure 2a). Such a structure is probably due to the presence of nitrogen.[21,25] The outer-wall diameter of CNTs ranges from 6 to 50 nm, which is composed of 6−30 concentric graphite shells, i.e., multiwalled (Figure 2e), depending on the thickness of the Fe film and the size of the Fe clusters. Iron particles were found enclosed within the ends of the CNTs (Figure 2b), which were identified by the EELS. From the SEM image shown in the ellipse in Figure 1e and the direction of the "bamboo" structures, it can be concluded that CNTs were grown via the base growth mechanism. Figure 2, parts c and d, shows the smallest carbon nanotubes produced in this work, i.e., 6 nm in diameter, when deposited on 1 nm Fe film. This CNT is composed of some amorphous structures within the graphitic shells, in contrast to the well-ordered graphitic shells (Figure 2b) of the CNTs with larger outer-wall diameters. The presence of amorphous structure could be explained by the fast growth rate such that carbon atoms did not have enough diffusion time to complete the construction of graphitic shells or it can be considered as the one of the growing stage before complete shells or tubes could be grown.

To investigate the cause of the formation of the amorphous structures, EELS and FTIR were carried out for structural and compositional analyses. Figure 3 part a and b, shows the near-edge EELS spectrum of carbon K-edge of well-ordered CNT

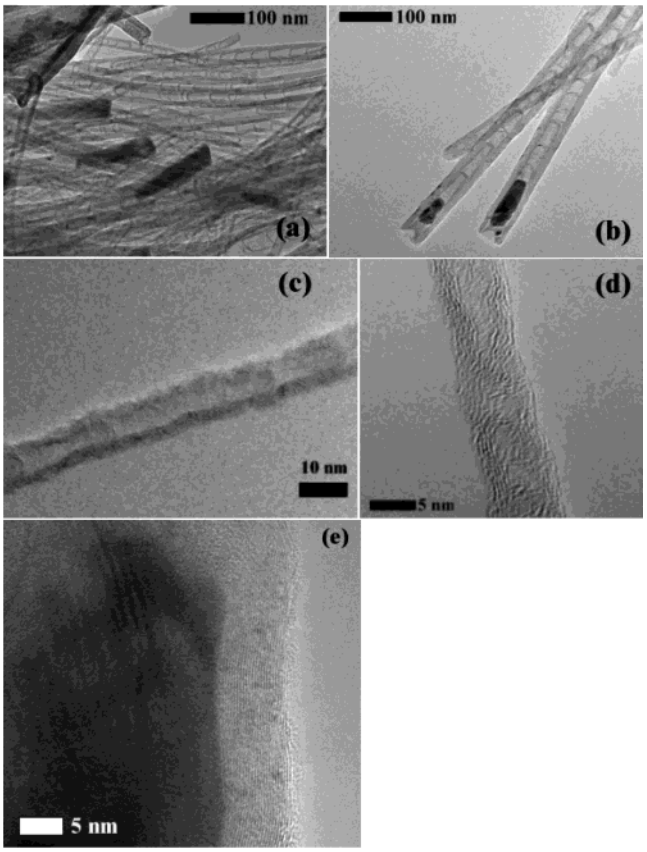

Figure 2. TEM of CNTs showing (a) almost all the CNTs have a "bamboo"-type or polymerized nanobell structure, (b) base growth mechanism revealed by the "direction" of the "bamboo"-type structures, (c) and (d) the smallest CNTs with an outer-wall diameter of ~6 nm have some amorphous characters, and (e) multiwalled structure of CNTs.

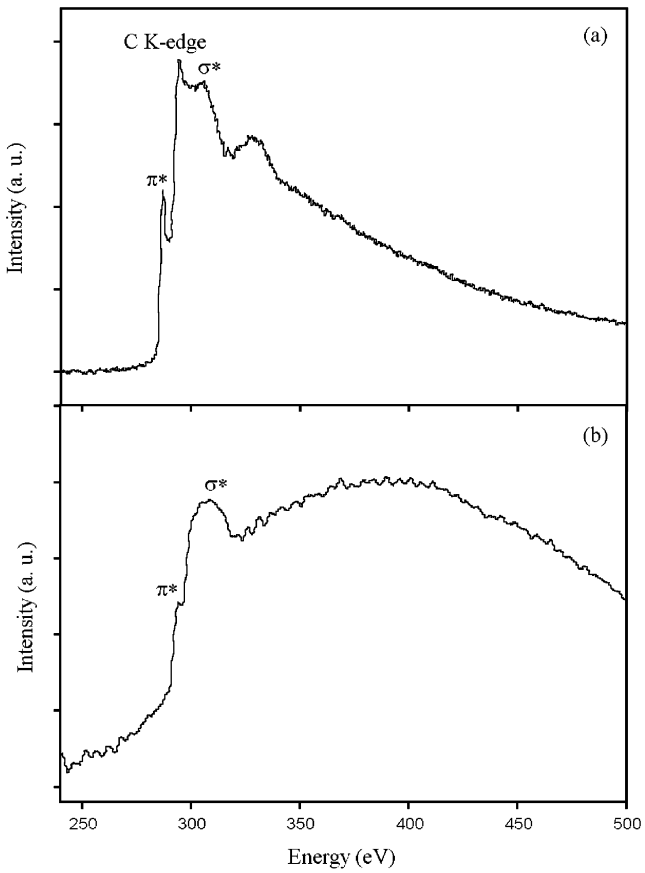

Figure 3. Carbon K-edge near-edge EELS spectrum of CNTs, (a) well-ordered CNT, (b) amorphous CNT.

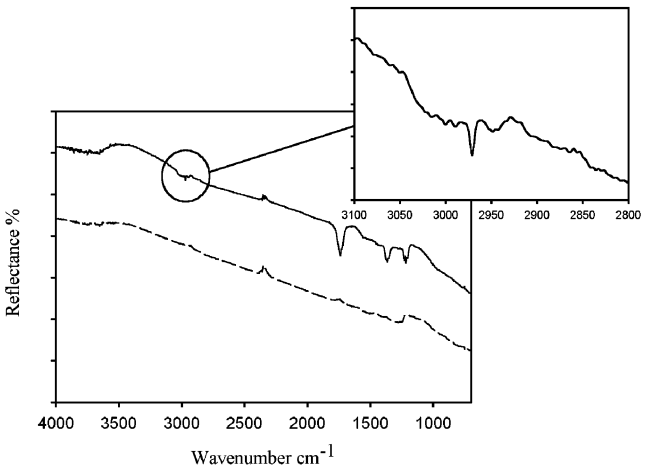

Figure 4. FTIR spectra of well-ordered CNTs (dash line) and amorphous CNTs (solid line).

(Figure 2b) and amorphous CNT (Figure 2c), respectively. It is clearly revealed that well-ordered CNT shows a carbon K-edge peak and a sharp π^* peak, which appears at 285 eV, giving evidence that the carbon atoms have sp^2 hybridization, i.e., graphitic structures, in the EELS spectrum (Figure 3a).[16] In contrast, amorphous CNT (Figure 3b) shows very low π^* signal; moreover, instead of a sharp carbon K-edge peak, a broad σ^* peak was observed. This indicates the presence of amorphous structures, which were mostly comprised of sp^3 bonding. The nature of sp^3 bonding was revealed by FTIR. Figure 4 shows the FTIR spectra of well-ordered CNTs (dash line) and amorphous CNTs (solid line). Peaks at 2900−3050 cm^{-1} were observed only in amorphous CNTs, and were assigned to C−H bonding. This suggests the possibility of the incorporation of hydrogen during the growth of CNTs.

Figure 3a also reveals that there is no detectable nitrogen EELs signal (401 eV) in the CNTs. XPS analysis also confirmed that no detectable CN_x compound was found since no nitrogen content was detected in the survey (Figure 5). Same observations were obtained for all samples.

Figure 6 shows measurements of the current density J (mA/cm^2) against local applied field E (V/μm) for the CNTs grown on 1 nm thick iron films on silicon substrate, which were measured at four different tip-to-sample distances d, i.e., 100, 150, 200 and 250 μm. From this figure, it shows that four curves have almost the same J−E characteristics, which reveal a linear relation between the anode voltage and distance. The FEE turn-on and threshold fields were found to be 3.5 V/μm (for 10 μA cm^{-2}) and 4.5 V/μm (for 10 mA cm^{-2}), respectively. These values were lower than those for CNTs grown on 2 and 5 nm iron films (not shown here). The reason should be due to the higher aspect ratio (smaller diameter and longer length) as well as better alignment of the CNTs grown on 1 nm thick iron films than those of the other two cases. Figure 6 also shows that a current density of 0.63 A cm^{-2} can be obtained when the electric field is 7.5 V/μm.

The present results show that pure and well-aligned CNTs can be synthesized by microwave plasma CVD by using N_2 and NH_3 as carrier gases and CH_4 as a deposition gas. To investigate the role of N_2 and NH_3 in the growth process, we have performed two other tests, where one of them was eliminated during growth. We found that, without N_2 gas, no

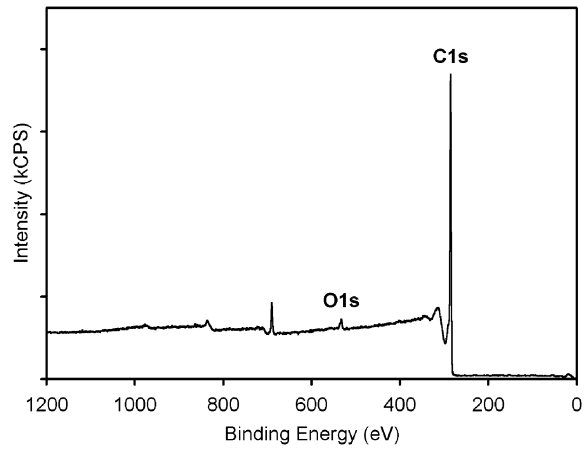

Figure 5. XPS spectrum of the CNTs.

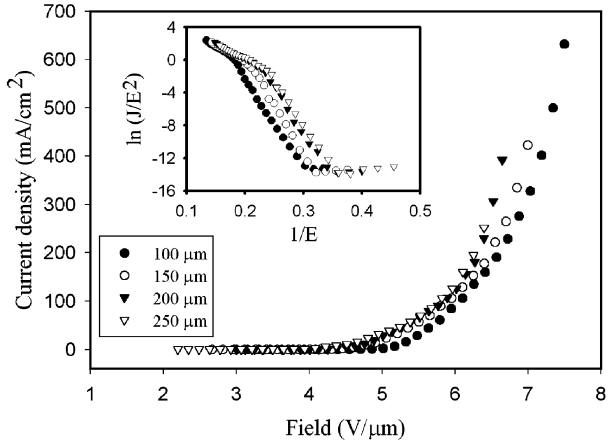

Figure 6. Plots of field emission current density J (mA/cm^2) against local applied field E (V/μm) for the CNTs grown on the 1 nm thick iron films on silicon substrate. The measurements were taken at four anode-to-sample distances (d = 100, 150, 200, and 250 μm). The inset shows the corresponding Fowler-Nordheim plots.

CNTs could be grown with the same NH_3 to CH_4 gas ratio at the same pressure. This suggested that N_2 could have the role of diminishing the hydrogen-containing etching species in the plasma. On the other hand, without NH_3 gas, curly CNTs were grown with poor alignment. This suggested that the NH_x species contributed to the alignment of CNTs. Nevertheless, the CNTs did not show any CN_x compound or nitrogen when examined by EELS and XPS.

Conclusions

Well-aligned multiwalled carbon nanotubes were grown by the microwave plasma-enhanced CVD method. We showed that pure carbon nanotubes could be grown by using nitrogen as the only carrier gas without ammonia, while pure and well-aligned carbon nanotubes could be grown only by adding a small amount of ammonia gas in the nitrogen gas (with gas ratio N_2/NH_3 = 50:2 in this work). In both cases, pure carbon nanotubes containing no detectable CN_x or nitrogen-containing compounds can be fabricated. This opens a possibility to fabricate pure and well-aligned carbon nanotubes using the inexpensive and nontoxic nitrogen chemistry rather than ammonia and hydrogen chemistry. The formation of amorphous structures in the "smallest" carbon nanotubes suggests the possibility of hydrogen incorporation during growth of carbon nanotubes, and a new direction in studying the nucleation and growth mechanisms of carbon nanotubes. Field electron emission measurements revealed that these pure carbon nanotubes exhibit excellent electron emission, and may be useful for practical applications such as flat panel display and other electronic devices.

The work described in this paper was fully supported by grants from CityU [7001405 and 7001390].

References and Notes

(1) Bower, C.; Zhu, W.; Shalom, D.; Lopez, D.; Chen, L. H.; Gammel, P. L.; Jin, S. *Appl. Phys. Lett.* **2002**, *80*, 3820.
(2) Liu, C.; Yang, Q. H.; Tong, Y.; Cong, H. T.; Cheng, H. M. *Appl. Phys. Lett.* **2002**, *80*, 2389.
(3) Larsen, T.; Moloni, K.; Flack, F.; Eriksson, M. A.; Lagally, M. G.; Black, C. T. *Appl. Phys. Lett.* **2002**, *80*, 1996.
(4) Yenilmez, E.; Wang, Q.; Chen, R. J.; Wang, D.; Dai, H. *Appl. Phys. Lett.* **2002**, *80*, 2225.
(5) Ritschel, M.; Uhlemann, M.; Gutfleisch, O.; Leonhardt, A.; Graff, A.; Täschner, Ch.; Fink, J. *Appl. Phys. Lett.* **2002**, *80*, 2985.
(6) Thostenson, E. T.; Li, W. Z.; Wang, D. Z.; Ren, Z. F.; Chou, T. W. J. *Appl. Phys.* **2002**, *91*, 6034.
(7) Kratschmer, W.; Lamb, L. D.; Fostiropoulos, K.; Huffman, D. R. *Nature* **1990**, *347*, 354.
(8) Ebbesen, T. W.; Ajayan, P. M. *Nature* **1992**, *358*, 16.
(9) Journet, C.; et al. *Nature* **1997**, *388*, 756.
(10) Smalley, R. *Science* **1996**, *273*, 483.
(11) Dai, H.; Rinzler, A. G.; Nikolaev, P.; Thess, A.; Colbert, D. T.; Smalley, R. E. *Chem. Phys. Lett.* **1996**, *260*, 471.
(12) Cassell, A. M.; Raymakers, J. A.; Kong, J.; Dai, H. J. *J. Phys. Chem. B* **1999**, *103*, 6484.
(13) Ren, Z. F.; Huang, Z. P.; Xu, J. W.; Wang, J. H.; Bush, P.; Siegal, M. P.; Provencio, P. N. *Science* **1998**, *282*, 1105.
(14) Bower, C.; Zhu, W.; Jin, S.; Werder, D. J.; Zhou, O. *Appl. Phys. Lett.* **2000**, *77*, 830.
(15) Bower, C.; Zhou, O.; Zhu, W.; Werder, D. J.; Jin, S. *Appl. Phys. Lett.* **2000**, *77*, 2767.
(16) Zhong, D.; Liu, S.; Zhang, G.; Wang, E. G. *J. Appl. Phys.* **2001**, *89*, 5939.
(17) Murakami, H.; Hirakawa, M.; Tanaka, C.; Yamakawa, H. *Appl. Phys. Lett.* **2000**, *76*, 1776.
(18) Zhang, Y.; Chang, A.; Cao, J.; Wang, Q.; Kim, W.; Li, Y.; Morris, N.; Yenilmez, E.; Kong, J.; Dai, H. *Appl. Phys. Lett.* **2001**, *79*, 3155.
(19) Avigal, Y.; Kalish, R. *Appl. Phys. Lett.* **2001**, *78*, 2291.
(20) Dai, H. *Appl. Phys. A* **2001**, *80*, 29.
(21) Ma, X.; Wang, E. G. *Appl. Phys. Lett.* **2001**, *78*, 978.
(22) Wong, W. K.; Meng, F. Y.; Li, Q.; Au, F. C. K.; Bello, I.; Lee, S. T. *Appl. Phys. Lett.* **2002**, *80*, 877.
(23) Zhu, W.; Bower, C.; Zhou, O.; Kochanski, G.; Jin, S. *Appl. Phys. Lett.* **1999**, *75*, 873.
(24) Sohn, J. I.; Choi, C.; Lee, S.; Seong, T. *Appl. Phys. Lett.* **2001**, *78*, 3130.
(25) Cui, H.; Zhou, O.; Stoner, B. R. *J. Appl. Phys.* **2000**, *88*, 6072.